Earthquakes and Structures, *Vol. 14, No. 5 (2018) 459-465*
DOI: https://doi.org/10.12989/eas.2018.14.5.459

Softening and hardening tuned mass dampers

Mohammad Khalil Khalili* and Karim Badamchi[a]

Department of Civil Engineering, University of Tabriz, 29 Bahman Blvd, Tabriz 51666-16471, Iran

(Received June 25, 2017, Revised March 5, 2018, Accepted March 19, 2018)

Abstract. Reducing response of buildings during earthquakes by mass dampers, has been examined in many articles and books. Nowadays, many researchers are trying to realistically examine this type of dampers by new methods of performance. In this paper, for the better study of tuned mass damper (TMD), two schematic models are presented for a passive TMD with softening stiffness (softening TMD) and a passive TMD with hardening stiffness (hardening TMD). Then by modeling and analysis of the damper on a single degree of freedom (SDOF) structure and an 11-story steel building, the dampers performance was evaluated. State space was used for damper and structure modeling and to solve nonlinear equations, the Newton-Raphson method was used. The results show that when the structure is subjected to the Chi-Chi earthquake, response of the sixth floor in the system without TMD reduces 54.0% in comparison to the structure with softening TMD. This percentage of reduction for hardening TMD is 55.0%. Also for the Tabas earthquake, reduction in the RMS acceleration of the sixth floor in the system with hardening TMD is 96.2% more than the structure without TMD. This percentage of reduction for hardening TMD is 96.3%.

Keywords: softening damper; hardening damper; tuned mass damper; geometrically nonlinear behaviour; nonlinear analyses

1. Introduction

The effectiveness of mass dampers has been proven in both theory and practice (Kareem *et al.* 1999, Soto and Adeli 2013). Appropriate TMD stiffness and damping parameters should be selected according to the mass of the TMD (mTMD) and the main structural characteristics, with favourable relations with which to find these values provided by Sadak *et al.* (1997). The latter researchers offered Eqs. (1)-(2) for determining the damping and stiffness factors of TMDs according to the ratio of the mTMD to the mass of the SDOF structure

$$f = \frac{1}{1+\mu}\left[1-\beta\sqrt{\frac{\mu}{1+\mu}}\right] \tag{1}$$

$$\xi = \frac{\beta}{1+\mu} + \sqrt{\frac{\mu}{1+\mu}} \tag{2}$$

In these relations, μ is the ratio of the mTMD to the mass of the structure, β is the damping ratio of the structure, f is the ratio of the frequency of the TMD to the frequency of the structure, and ξ is the damping ratio of the damper.

TMD efficiency can be increased via the use of either active or semi-active methods. In an active system, a controller is added that enables the damper to apply the appropriate force to the structure at each moment in time (Soleymani and Khodadadi 2014). This type of damper operates well against the forces of hurricane, wind and earthquake (He and Li 2014, Pourzeynali *et al.* 2007, Soleymani and Khodadadi 2014). In semi-active systems, stiffness and/or damping can be changed at any moment according to the external force on the building (Bajkowski *et al.* 2016, Das *et al.* 2012, Ghaffarzadeh *et al.* 2012). Here the controller determines the amount of appropriate stiffness and/or damping, based on the written control algorithm. There are several methods available with which to design a semi-active stiffness system, for example using a single mass with a variable stiffness spring, adaptive-length pendulum semi-active TMDs, TMDs with resettable variable stiffness, and TMDs with a folding variable stiffness spring (Lin *et al.* 2015, Nagarajaiah 2009, Rafieipour *et al.* 2014, Varadarajan and Nagarajaiah 2004). Following on from articles evaluating the manner and use of nonlinear viscous damping for structures, some recent research has investigated the associated relationships and how to solve equation presentation (Lin *et al.* 2015, Shum 2015).

Assadi and Farshi (2011) used a set of linear springs to create a TMD with nonlinear stiffness. These springs are connected together in such a way that they each exhibit nonlinear behaviour in themselves. Eason *et al.* (2013) used a semi-active TMD to improve the performance of an existing TMD in a structure, with the new damper connected to the primary damper in series. Viet and Nghi (2014) introduced a nonlinear TMD with two degrees of freedom: one rotational and the other transitional in the bar direction. The authors stated that the regulating frequencies of these dampers for swing and translational motions should be close to the main frequency and the second frequency of

*Corresponding author, Ph.D. Student
E-mail: Khalili@tabrizu.ac.ir
[a]Assistant Professor
E-mail: k.badamchi@tabrizu.ac.ir

Copyright © 2018 Techno-Press, Ltd.
http://www.techno-press.com/journals/eas&subpage=7 ISSN: 2092-7614 (Print), 2092-7622 (Online)

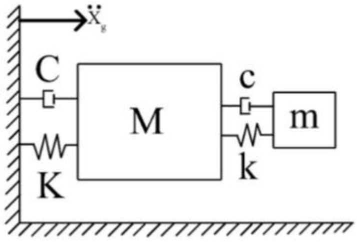

Fig. 1 Structure with TMD

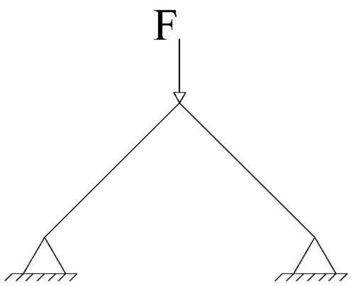

Fig. 2 Softening and hardening system

the main structure, respectively, with numerical solutions also offered. Sun *et al.* (2014) conducted an experimental investigation of a SDOF structure with both a nonlinear TMD and an adaptive pendulum TMD. It was found that the adaptive pendulum TMD not only improved the performance of the initial structure but also improved the performance of the nonlinear TMD.

Ductility and hardening factors have recently become the focus of intense research in civil-earthquake engineering. With regard to this issue, in the present paper two new functional models for nonlinear TMDs are presented, with the modelling method and solutions to the nonlinear dynamic equations discussed. The two models proposed are as follows: TMD with softening nonlinear stiffness and TMD with hardening nonlinear stiffness. These systems and the selected structure are then modelled in state space and the obtained nonlinear dynamic equations solved via the Newton-Raphson method.

2. Introduction of the proposed models

A TMD is a combination of its mass and specific stiffness and damping values. Fig. 1 depicts a damper connected to a SDOF system, where M, C and K are respectively the mass, damping and stiffness of the structure and m, c and k are respectively the mass, damping and stiffness of the damper.

To create a nonlinear TMD, geometric softening and hardening of the members can be used. Hardening of the system displayed in Fig. 2 takes place when it is stretched under the influence of vertical load, while softening takes place under compression.

Due to this issue, TMD softening and hardening systems can be employed, as shown in Figs. 3-4, respectively.

3. Equations of motion for the structure and solving method for nonlinear equations

When a building is affected under the influence of seismic loads, the equations of motion for the structure in the state space are expressed as in Eq. (3).

$$\begin{Bmatrix} \{\dot{u}\} \\ \{\ddot{u}\} \end{Bmatrix} = \begin{bmatrix} O_{n\times n} & I_{n\times n} \\ -[M]^{-1}[K] & -[M]^{-1}[C] \end{bmatrix} \begin{Bmatrix} \{u\} \\ \{\dot{u}\} \end{Bmatrix} + \begin{bmatrix} O_{n\times n} \\ I_{n\times n} \end{bmatrix} \{r\}\ddot{u}_g(t) \tag{3}$$

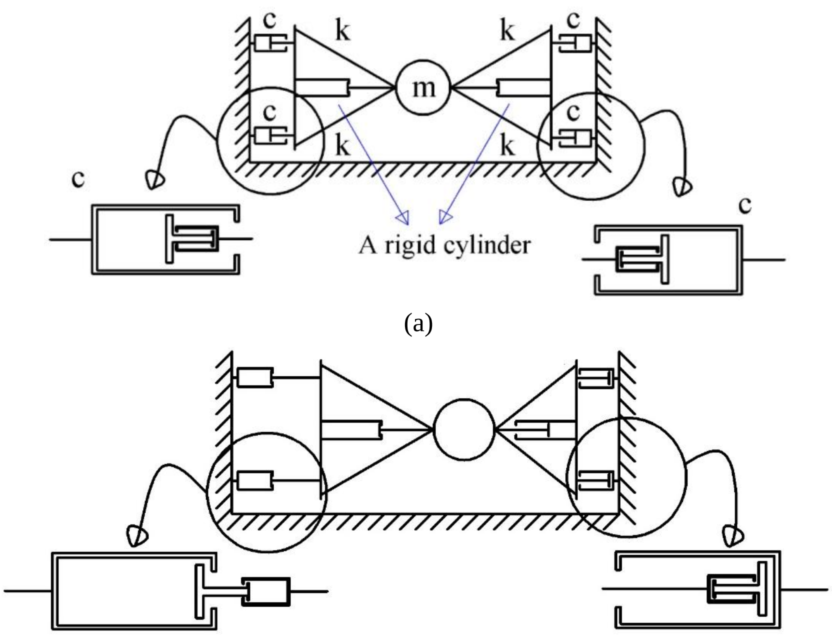

(a)

(b)

Fig. 3 (a) Schematic model of a softening TMD; (b) Softening TMD under seismic loading

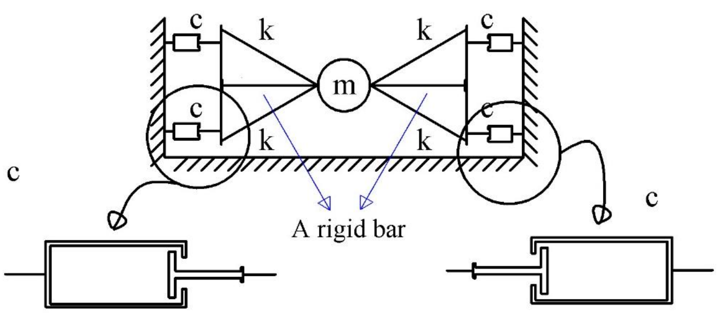

(a)

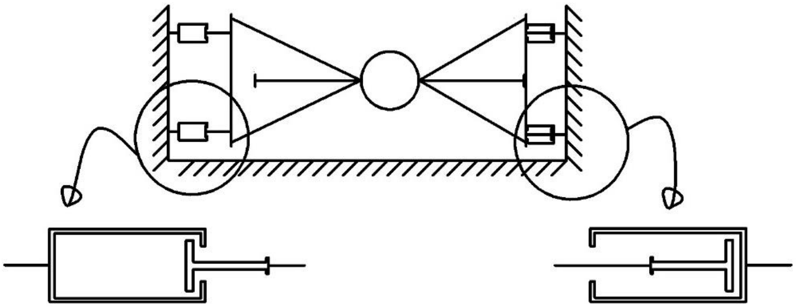

(b)

Fig. 4 (a) Schematic model of a hardening TMD; (b) Hardening TMD under seismic loading

where [M], [K] and [C] are the mass, stiffness and damping matrix of the structure, respectively, vectors u, I and O are the displacement, unit and zero matrixes, respectively, and $\{r\}$ is a $1\times n$ vector such that all its elements are equal to 1 for ordinary structures.

Equations of motion for a structure with a damper are similar to Eq. (1), with the difference being that one degree is added to the degrees of freedom system.

The stiffness matrix of any ductile member of the TMD is also expressed as in Eq. (4).

$$K=\frac{EA}{L}\begin{bmatrix} C^2 & CS & -C^2 & -CS \\ CS & S^2 & -CS & -S^2 \\ -C^2 & -CS & C^2 & CS \\ -CS & -S^2 & CS & S^2 \end{bmatrix} \tag{4}$$

where C represents $Cos\Theta$, S indicates $Sin\Theta$, Θ is the angle between the member and the horizontal axis, and E, A and L are Young’s modulus, member cross-sectional area and member length, respectively.

When a structure is subjected to seismic loads, the above equations can be solved using conventional methods. However, when a structure has a nonlinear stiffness, a method such as Euler, Runge-Kutta or Newton-Raphson should be used to correct the nonlinear factor in solving the equations. In the present study, the Newton-Raphson method was used to solve the nonlinear equations. According to the Newton-Raphson method, after solving the equations in linear mode the internal force of each member is found, followed by the difference between the external force and the resistant internal force; a new stiffness value is calculated during this step. Based on the new stiffness value and unbalancing force, the equations of motion are formulated and solved, with this loop repeated until convergence is achieved. It should be noted that due to the many changes in length, the angle between the ductile members and horizon will change and consequently the stiffness will also vary at any moment in time.

Fig. 5 shows the process of solving equations carried out using the Newton-Raphson method.

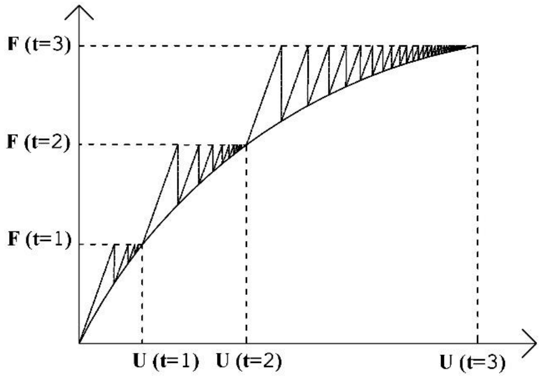

(a) Newton-Raphson with initial stiffness

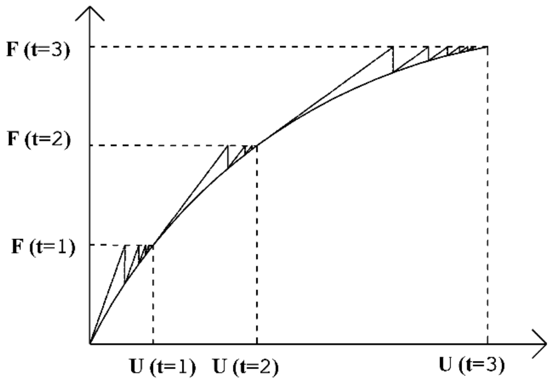

(b) Updating of Newton-Raphson at each time increment

Fig. 5 Newton-Raphson method (Oller 2014)

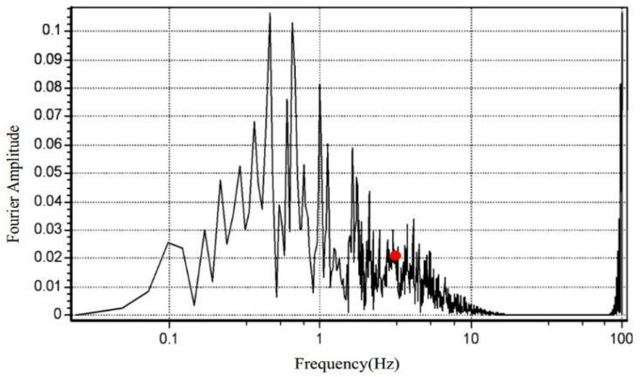

Fig. 6 Fourier amplitude spectrum for the Borrego earthquake

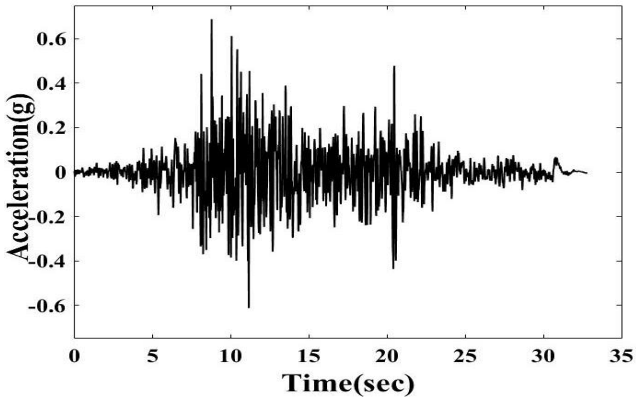

Fig. 7 Temporal history of Tabas earthquake acceleration

Table 1 Maximum displacement of structure (mm)

	Maximum displacement
Structure Without Damper	4.245
Structure With TMD	2.407
Structure with Softening TMD	2.405
Structure with Hardening TMD	2.409

4. The case study structure model

To check the proposed systems, the following sections describe a case study involving a SDOF system and a steel 11-storey building.

4.1 Single degree of freedom structure

At this stage a SDOF structure is examined for both the softening and hardening TMDs. This system and the designed passive dampers are in accordance with (Sadek *et al.* 1997), i.e., the SDOF system has a period of 0.25s, a damping ratio of 0.02, and the ratio of the damper mass and fundamental frequency to the mass and fundamental frequency of the main system are 0.1 and 0.9036, respectively. These systems are here modelled as being subjected to the Borrego earthquake, with the Fourier amplitude spectrum shown in Fig. 6.

The results of the analyses are displayed in Table 1.

In Eq. (2), the initial values of L, EA/L and Θ are respectively 1 m, 25.785 N/m and 45° for each member of the damper. The results obtained in the present study exhibit only minor differences with those reported in (Sadek *et al.* 1997), in which both a structure without damper and a structure with TMD were analyzed. Furthermore, the softening TMD performed better than the linear TMD and hardening TMD.

The same structure was then subjected to both the Borrego and Tabas earthquakes for Θ values of 5°, 15°, 30°, 45°, 60°, 75° and 85°. In these scenarios, the initial length of members, stiffness and damping of the dampers were selected according to the first case study. The temporal history of Tabas earthquake acceleration is shown in Fig. 7.

The results of the second scenario are shown in Tables 2-3.

As can be seen in Tables 2-3, for values of Θ above 60° the speed of maximum displacement changes is higher and thus in practice the risk of using these angles is greater. For values of Θ below 60°, whereas for the Borrego earthquake simulation the softening TMD system performed better, for the Tabas earthquake simulation the hardening TMD system performed better. Using the Fourier spectrum of each earthquake, the total energy per mass unit can be examined for different earthquakes to determine the effect of softening and hardening.

For Θ=60° in the Borrego earthquake scenario, the softening and hardening systems respectively reduced maximum displacement by 43.38% and 43.22% in comparison to the structure without damper. For the Tabas earthquake scenario these values were lower at 27.72% and 27.96%, respectively.

Table 2 Maximum displacement of structure for the Borrego earthquake (mm)

Degree	Θ=5°	Θ=15°	Θ=30°	Θ=45°	Θ=60°	Θ=75°	Θ=85°
Structure Without Damper	4.245	4.245	4.245	4.245	4.245	4.245	4.245
Structure with Softening TMD	2.407	2.4068	2.4063	2.4054	2.4037	2.3991	2.383
Structure with Hardening TMD	2.407	2.4071	2.4076	2.4085	2.4102	2.4147	2.4322

Table 3 Maximum displacement of structure for the Tabas earthquake (cm)

Degree	Θ=5°	Θ=15°	Θ=30°	Θ=45°	Θ=60°	Θ=75°	Θ=85°
Structure Without Damper	1.8826	1.8826	1.8826	1.8826	1.8826	1.8826	1.8826
Structure with Softening TMD	1.3587	1.3588	1.3591	1.3597	1.3608	1.3637	1.375
Structure with Hardening TMD	1.3587	1.3586	1.3582	1.3575	1.3562	1.3593	1.3774

Table 4 Characteristics of the simulated 11-storey building

Number of Story	Mass of Story (KN.s/m)	Stiffness of Story (MN/m)
11	176	312
10	203	437
9	203	437
8	203	437
7	201	450
6	201	450
5	201	450
4	200	450
3	201	468
2	201	476
1	215	468

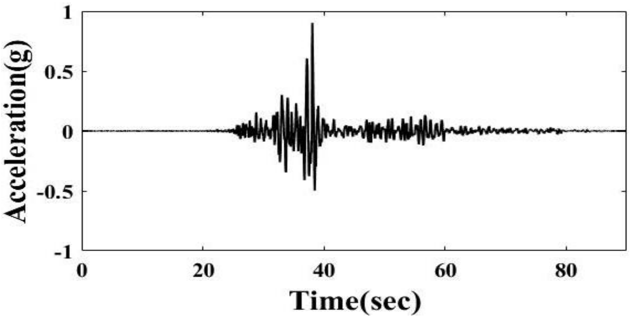

Fig. 8 Temporal history of Chi-Chi Taiwan earthquake acceleration

4.2 Multi degrees of freedom structure

In this section an 11-storey structure is evaluated, with the characteristics of this structure detailed in Table 4.

The damping for the structure was calculated using the Rayleigh method (Pourzeynali *et al.* 2007). the damping ratio of 1% was used for this building. To create the damper, the top floor was used (Chey *et al.* 2010a, b; Zahrai *et al.* 2013), with the stiffness and damping of the damper set at 6402500 N/m and 619340 N.sec/m, respectively (Sadek *et al.* 1997). In Eq. (2), the initial values of L, EA/L and Θ were respectively set at 10 m, 3201250 N/m and 60° for each member of the damper. The modelled structure and damper systems were then subjected to Chi-Chi and Tabas earthquake scenarios. The temporal history of Chi-Chi earthquake acceleration is shown in Fig. 8.

The results of this analysis are shown in Tables 5-6. According to the results shown in Tables 5-6, the softening TMD was able to reduce the max displacement of the tenth, fifth and first floors of the structure in the Chi-Chi earthquake scenario by 54.2%, 54.2% and 54.7%, respectively, and in the Tabas earthquake scenario by 60.2%, 62.5% and 59.5%, respectively. In contrast, the hardening TMD was able to reduce max displacement for the tenth, fifth and first floors in the Chi-Chi earthquake scenario by 54.6%, 55.3% and 56.3%, respectively, and by 60.0%, 62.3% and 59.5% in the Tabas earthquake scenario. As can also be seen in the two tables, in both the Chi-Chi and Tabas earthquake scenarios the softening TMD itself, i.e., the eleventh floor, experienced less displacement than the hardening TMD. The displacement record of the structure's tenth floor under the Chi-Chi and Tabas earthquakes is shown in Figs. 9-10, respectively.

A decrease in RMS displacement reduces the effects of fatigue failure on structure members, providing reassurance for potential residents. As can be seen in the figures, TMD application considerably reduces displacement at any moment in time. For example, analysis of Tables 5-6 reveals that when the modelled structures were subjected to the Chi-Chi earthquake scenario, RMS displacement of the tenth floor in the structure without TMD, with softening TMD and with hardening TMD was equal to 4.72 cm, 0.27 cm and 0.25 cm, respectively. In the Tabas earthquake scenario these values were equal to 1.22 cm, 0.04 cm and 0.04 cm, respectively.

5. Conclusions

As technology advances, engineers are able to look for methods with which to increase project safety factor values and at the same time ensure their economic viability. One such method designed to achieve the above objectives is the use of softening and hardening TMDs. In this paper two functional models for a softening TMD and hardening TMD

Table 5 RMS and maximum displacement of floors for the Chi-Chi earthquake scenario (cm)

Number of Story	Without Damper		Softening Damper		Hardening Damper	
	RMS	Displacement	RMS	Displacement	RMS	Displacement
1	0.0872	14.2625	0.0055	6.4664	0.0048	6.2333
2	0.3361	28.0431	0.0211	12.7030	0.0183	12.2931
3	0.7369	41.5696	0.0461	18.8529	0.0401	18.3073
4	1.2807	54.8445	0.0796	24.9675	0.0696	24.3072
5	1.9133	67.0490	0.1180	30.6920	0.1038	29.9444
6	2.5861	77.9300	0.1581	35.8671	0.1400	35.0683
7	3.2473	87.2809	0.1966	40.2985	0.1755	39.5167
8	3.8647	95.1695	0.2312	43.9357	0.2084	43.2195
9	4.3694	101.1524	0.2579	46.5447	0.2351	45.9546
10	4.7210	105.1097	0.2743	48.0912	0.2535	47.6989
11	4.9601	107.7153	0.8001	81.5588	1.0657	93.6801

Table 6 RMS and maximum displacement of floors for the Tabas earthquake scenario (cm)

Number of Story	Without Damper		Softening Damper		Hardening Damper	
	RMS	Displacement	RMS	Displacement	RMS	Displacement
1	0.0229	3.5398	0.0010	1.4339	0.0010	1.4337
2	0.0878	6.7737	0.0038	2.6524	0.0037	2.6534
3	0.1917	9.6950	0.0079	3.6527	0.0077	3.6571
4	0.3318	12.5177	0.0131	4.6480	0.0129	4.6756
5	0.4943	15.2124	0.0190	5.7009	0.0187	5.7336
6	0.6668	17.9458	0.0253	6.7402	0.0249	6.7756
7	0.8364	20.0732	0.0314	7.7987	0.0310	7.8350
8	0.9951	21.8978	0.0372	8.8932	0.0368	8.9318
9	1.1254	23.8716	0.0421	9.6860	0.0417	9.7286
10	1.2167	25.4408	0.0454	10.1265	0.0451	10.1729
11	1.2793	26.5394	0.1689	17.7725	0.1779	17.9439

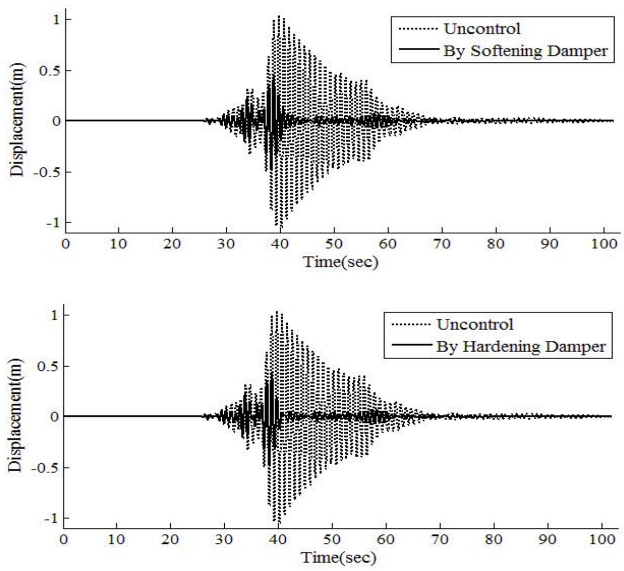

Fig. 9 Displacement of the tenth floor in the ChiChi earthquake scenario

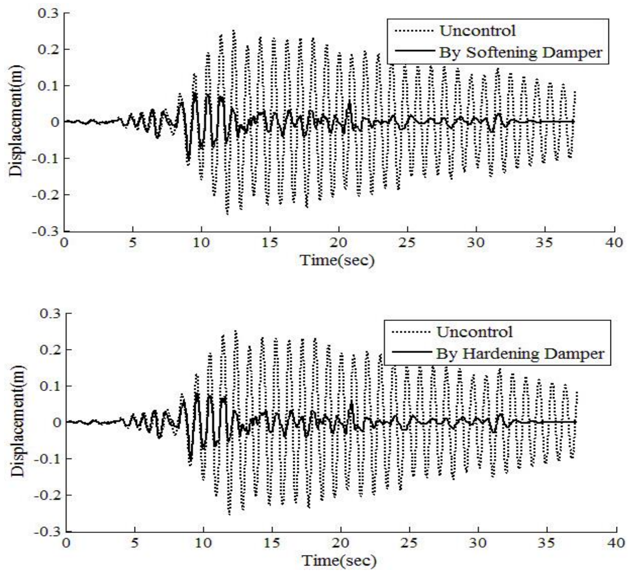

Fig. 10 Displacement of the tenth floor in the Tabas earthquake scenario

were introduced, with the behaviour of the two dampers and the associated structure studied at the onset of two earthquake scenarios. The results showed that in the Tabas earthquake scenario, the softening TMD and hardening TMD reduced the maximum floor displacement by an average of 58.50% and 58.32%, respectively, and the average RMS displacement by 95.24% and 95.21%, respectively, in comparison to the structure without damper.

Acknowledgments

The authors would like to thank all who gave support to this effort especially Dr. Majid Barghian.

References

Bajkowski, J.M., Dyniewicz, B. and Bajer, C.I. (2016), "Semi-active damping strategy for beams system with pneumatically controlled granular structure", *Mech. Syst. Signal Pr.*, **70**, 387-396.

Chey, M.H., Chase, J.G., Mander, J.B. and Carr, A.J. (2010a), "Semi-active tuned mass damper building systems: application", *Earthq. Eng. Struct. D.*, **39**(1), 69-89.

Chey, M.H., Chase, J.G., Mander, J.B. and Carr, A.J. (2010b), "Semi-active tuned mass damper building systems: design", *Earthq. Eng. Struct. D.*, **39**(1), 119-139.

Das, D., Datta, T. and Madan, A. (2012), "Semiactive fuzzy control of the seismic response of building frames with MR dampers", *Earthq. Eng. Struct. D.*, **41**(1), 99-118.

Eason, R., Sun, C., Dick, A. and Nagarajaiah, S. (2013), "Attenuation of a linear oscillator using a nonlinear and a semi-active tuned mass damper in series", *J. Sound Vib.*, **332**(1), 154-166.

Farshi, B. and Assadi, A. (2011), "Development of a chaotic nonlinear tuned mass damper for optimal vibration response", *Commun. Nonlin. Sci.*, **16**(11), 4514-4523.

Ghaffarzadeh, H., Dehrod, E.A. and Talebian, N. (2013), "Semi-active fuzzy control for seismic response reduction of building frames using variable orifice dampers subjected to near-fault earthquakes", *J. Vib. Control*, **19**(13), 1980-1998.

He, Y.C. and Li, Q. (2014), "Dynamic responses of a 492-m-high tall building with active tuned mass damping system during a typhoon", *Struct. Control Hlth. Monit.*, **21**(5), 705-720.

Kareem, A., Kijewski, T. and Tamura, Y. (1999), "Mitigation of motions of tall buildings with specific examples of recent applications", *Wind Struct*., **2**(3), 201-251.

Lin, G.L., Lin, C.C., Chen, B.C. and Soong, T.T. (2015), "Vibration control performance of tuned mass dampers with resettable variable stiffness", *Eng. Struct*., **83**, 187-197.

Lin, J.L., Liu, T.H. and Tsai, K.C. (2015), "Real-valued modal response history analysis for asymmetric-plan buildings with nonlinear viscous dampers", *Soil Dyn. Earthq. Eng*., **77**, 97-110.

Nagarajaiah, S. (2009), "Adaptive passive, semiactive, smart tuned mass dampers: identification and control using empirical mode decomposition, Hilbert transform, and short-term Fourier transform", *Struct. Control Hlth. Monit*., **16**(7-8), 800-841.

Oller, S. (2014), *Nonlinear Dynamics of Structures*, Springer, New York, USA.

Pourzeynali, S., Lavasani, H. and Modarayi, A. (2007), "Active control of high rise building structures using fuzzy logic and genetic algorithms", *Eng. Struct*., **29**(3), 346-357.

Rafieipour, M.H., Ghorbani-Tanha, A.K., Rahimian M and Mohammadi-Ghazi R (2014), "A novel semi-active TMD with folding variable stiffness spring", *Earthq. Eng. Eng. Vib*., **13**(3), 509-518.

Sadek, F., Mohraz, B., Taylor, A.W. and Chung, R.M. (1997), "A method of estimating the parameters of tuned mass dampers for seismic applications", *Earthq. Eng. Struct. D*., **26**(6), 617-636.

Shum, K. (2015), "Tuned vibration absorbers with nonlinear viscous damping for damped structures under random load", *J. Sound Vib*., **346**, 70-80.

Soleymani, M. and Khodadadi, M. (2014), "Adaptive fuzzy controller for active tuned mass damper of a benchmark tall building subjected to seismic and wind loads", *Struct. Des. Tall Spec*., **23**(10), 781-800.

Soto, M.G. and Adeli, H. (2013), "Tuned mass dampers", *Arch. Comput. Meth. E*., **20**(4), 419-431.

Sun, C., Nagarajaiah, S. and Dick, A. (2014), "Experimental investigation of vibration attenuation using nonlinear tuned mass damper and pendulum tuned mass damper in parallel", *Nonlin. Dyn*., **78**(4), 2699-2715.

Varadarajan, N. and Nagarajaiah, S. (2004), "Wind response control of building with variable stiffness tuned mass damper using empirical mode decomposition/Hilbert transform", *J. Eng. Mech*., **130**(4), 451-458.

Viet, L. and Nghi, N. (2014), "On a nonlinear single-mass two-frequency pendulum tuned mass damper to reduce horizontal vibration", *Eng. Struct*., **81**, 175-180.

Zahrai, S.M., Zare, A., Khalili, M.K. and Asnafi, A. (2013), "Seismic design of fuzzy controller for semi-active tuned mass dampers using top stories as the mass", *Asian J. Civil Eng. (BHRC)*, **14**(3), 383-396.

CC